ELSEVIER

Available online at www.sciencedirect.com

ScienceDirect

Journal of Organometallic Chemistry 692 (2007) 4139–4146

Journal of Organometallic Chemistry

www.elsevier.com/locate/jorganchem

Iridium(I) complex of chelating pyridine-2-thiolate ligand: Synthesis, reactivity, and application to the catalytic *E*-selective terminal alkyne dimerization via C–H activation

Kenichi Ogata *, Akinori Toyota *

Graduate School of Engineering, Tokyo University of Agriculture and Technology, 2-24-16 Naka-cho, Koganei-shi, Tokyo 184-8588, Japan

Received 22 May 2007; received in revised form 20 June 2007; accepted 21 June 2007
Available online 24 June 2007

Abstract

A novel iridium(I) complex bearing a chelate-coordinated pyridine-2-thiolate ligand [Ir(η^2-SNC_5H_4)(PPh_3)$_2$] (**2**) was prepared by the reaction of iridium ethylene complex [IrCl(C_2H_4)(PPh_3)$_2$] (**1**) with lithium salt of pyridine-2-thiol (Li[SNC_5H_4]). On the treatment of iridium(I) complex **2** with chloroform, iridium(III) dichloro-complex [$IrCl_2$(η^2-SNC_5H_4)(PPh_3)$_2$] (**3**) was formed. Reactions of complex **2** with methyldiphenylsilane, acetic acid, and *p*-tolylacetylene afforded iridium(III) hydride complexes [IrH($SiMePh_2$)(η^2-SNC_5H_4)(PPh_3)$_2$] (**4**), [IrH(O_2CCH_3)(η^2-SNC_5H_4)(PPh_3)$_2$] (**5**), and [IrH(C≡C(*p*-tolyl))(η^2-SNC_5H_4)(PPh_3)$_2$] (**6**), respectively. Complex **2** catalyzed dimerization of terminal alkynes leading to enynes (**7**) with high *E*-selectivity via C–H bond activation.

Keywords: Iridium complex; Pyridine-2-thiolate; Hydride complex; Dimerization of alkyne

1. Introduction

Pyridine-2-thiolate has been used as supporting ligand for transition metal complexes because of the versatility in their coordination modes [1]. Neutral monodentate [2], anionic S-monodentate [3], chelating [4], and bridging [5] pyridine-2-thiolate complexes have been reported. In the chemistry of iridium, several S-monodentate and chelating pyridine-2-thiolate iridium complexes which are four- and six-coordinate structure [6] and Cp* iridium(III) complex bearing a chelating pyridine-2-thiolate ligand [Cp*Ir(η^2-SNC_5H_4)N_3] [7] were reported. Photolysis of the Cp*Ir complex [Cp*Ir(η^2-SNC_5H_4)N_3] gave a pyridine-1-imido-2-thiolato complex, in which one of the nitrogen atoms of the azido ligand has been inserted into the iridium-N(Py) bond. In case of bridging pyridine-2-thiolate complexes, binuclear iridium(I) complexes [Ir(μ-SNC_5H_4)L]$_2$ (L = COD, (CO)$_2$), generated from the reaction of [IrCl(COD)]$_2$ with lithium salt of pyridine-2-thiol, Li[SNC_5H_4], has been reported [8]. The binuclear iridium(I) complex [Ir(μ-SNC_5H_4)(CO)$_2$]$_2$ reacted with CH_3I or CH_2I_2 to give iridium(II) complexes [Ir_2(CH_3)I(μ-SNC_5H_4)$_2$(CO)$_4$] or [Ir_2(CH_2I)I(μ-SNC_5H_4)$_2$(CO)$_4$] through oxidative addition between two metal centers. The reaction of [Ir(OMe)(COD)]$_2$ with sterically hindered pyridine-2-thiol bearing *tert*-butyl group in the *ortho*-position generated S-bridging binuclear complex [Ir(μ-SNC_5H_3-*o*-^{t}Bu)(COD)]$_2$ [9].

Low valent iridium(I) complex bearing chelate-coordinated pyridine-2-thiolate ligand has not been reported, though many other transition metal complexes bearing chelate-coordinated pyridine-2-thiolate ligand has been reported. Chelating pyridine-2-thiolate ligand have an ability to act as a bifunctional ligand (hard N-donor and soft S-donor), and we had an interest in the chemistry of its four-coordinated iridium(I) complex.

In this paper, we describe synthesis and reactivity of an iridium(I) complex. In addition, the catalytic activity in dimerization of terminal alkynes is also described.

---

* Corresponding authors. Tel./fax: +81 42 388 7162.
E-mail addresses: kogata@cc.tuat.ac.jp (K. Ogata), a-toyota@cc.tuat.ac.jp (A. Toyota).

0022-328X/$ - see front matter © 2007 Elsevier B.V. All rights reserved.
doi:10.1016/j.jorganchem.2007.06.030

2. Experimental

2.1. General procedures

All manipulations involving air- and moisture-sensitive organometallic compounds were carried out under dry argon atmosphere, which was purified by SICAPENT (Merck Co., Inc.), by using a standard Schlenk tube or high vacuum techniques. Toluene, hexane, diethyl ether and THF were distilled over Na/benzophenone prior to use. Chloroform was distilled over CaH_2 prior to use. $[IrCl(ethylene)(PPh_3)_2]$ (**1**) [10], $[Ir(\mu\text{-}SNC_5H_4)(COD)]_2$ [8] were prepared according to the literature methods. Other reagents employed in this research were commercially available and used without further purification. The NMR spectra were recorded on a JEOL Delta-400 spectrometer at ambient temperature. ^1H NMR spectra and $^{13}C\{^1H\}$ NMR spectra were measured using Me_4Si as an internal reference, and $^{31}P\{^1H\}$ NMR spectra were measured using 85% H_3PO_4 as an external reference. All chemical shifts were recorded in ppm and all coupling constants were recorded in Hz. Fast atom bombardment (FAB) mass spectra were measured on a JEOL JMS-SX102 spectrometer using *m*-nitrobenzylalcohol as matrix. Elementary analyses were measured on a Perkin–Elmer 240C.

2.2. Preparation of iridium(I)pyridine-2-thiolate complex $[Ir(\eta^2\text{-}SNC_5H_4)(PPh_3)_2]$ (2)

A solution of ethylene complex $[IrCl(C_2H_4)(PPh_3)_2]$ (**1**) (276 mg, 0.35 mmol) in THF (5 mL) was cooled to −78 °C, and then a THF solution of $Li[SNC_5H_4]$, which was prepared by the reaction of the parent $H[SNC_5H_4]$ (41 mg, 0.37 mmol) with ^{n}BuLi (1.58 M in a hexane solution, 0.24 mL, 0.38 mmol) at −78 °C, was added. The mixture was allowed to warm to room temperature. After several hours, the volatiles were removed under reduced pressure. The residual solid was washed with hexane several times and then extracted with toluene. The filtrate was evaporated off under high vacuum to give red complex **2** (250 mg, 0.151 mmol, 85%). FAB mass (*m*/*z*): 827 ($[M]^+$). ^1H NMR (C_6D_6): δ 6.0–9.2 (m, Ph and Pyridine unit). $^{31}P\{^1H\}$ NMR (C_6D_6): δ 20.9 (d, $J_{pp} = 20.4$ Hz, PPh_3), 22.8 (d, $J_{pp} = 20.4$ Hz, PPh_3). Anal. Calc. for $C_{41}H_{34}IrNP_2S$: C, 59.55; H, 4.14; N, 1.69. Found: C, 59.07; H, 4.17; N, 1.61%.

2.3. Preparation of iridium(III)pyridine-2-thiolate complexes

2.3.1. Preparation of $[IrCl_2(\eta^2\text{-}SNC_5H_4)(PPh_3)_2]$ (3)

To solution of complex **2** (35 mg, 0.042 mmol) in toluene (3 mL), chloroform (0.1 mL, 1.25 mmol) was added at room temperature. After 1 h, the solvent was removed under high vacuum and the residue was recrystallized from CH_2Cl_2 and diethyl ether, affording yellow crystals of **3** (18 mg, 0.020 mmol, 47%). ^1H NMR ($CDCl_3$): δ 5.8–8.9 (m, Ph and Pyridine unit). $^{31}P\{^1H\}$ NMR ($CDCl_3$): δ −12.7 (s, PPh_3). Anal. Calc. for $C_{41}H_{34}Cl_2IrNP_2S \cdot 0.5CH_2Cl_2$: C, 53.01; H, 3.75; N, 1.49. Found: C, 53.44; H, 3.93; N, 1.52%.

2.3.2. Preparation of $[IrH(SiMePh_2)(\eta^2\text{-}SNC_5H_4)(PPh_3)_2]$ (4)

To solution of complex **2** (64 mg, 0.077 mmol) in toluene (5 mL), methyldiphenylsilane (16 μL, 0.080 mmol) was added at room temperature. After 5 min, the solvent was removed under high vacuum and the residue was washed with hexane (3 × 5 mL) and then dried in vacuo, giving yellow powder of **4** (50 mg, 0.049 mmol, 63%). ^1H NMR (C_6D_6): δ −19.60 (t, $J_{PH} = 16.5$ Hz, 1 H, Ir–H), 0.80 (s, 3H, CH_3), 6.8–8.5 (m, 39H, Ph and Py), $^{31}P\{^1H\}$ NMR (C_6D_6): δ 5.8 (s, PPh_3). Anal. Calc. for $C_{54}H_{48}IrNP_2SSi$: C, 63.26; H, 4.72; N, 1.37. Found: C, 63.38; H, 4.86; N, 1.40%.

2.3.3. Preparation of $[IrH(O_2CCH_3)(\eta^2\text{-}SNC_5H_4)(PPh_3)_2]$ (5)

To solution of complex **2** (54 mg, 0.065 mmol) in toluene (5 mL), acetic acid (5 μL, 0.087 mmol) was added at room temperature. After 5 min, the solvent was removed under high vacuum and the residue was washed with hexane (3 × 5 mL) and then dried in vacuo, giving yellow powder of **5** (52 mg, 0.059 mmol, 90%). ^1H NMR (CD_2Cl_2): δ −17.53 (dd, $^2J_{P1H} = 16.8$ Hz, $^2J_{P2H} = 20.2$ Hz, 1 H, Ir–H), 1.12 (s, 3H, CH_3), 2.8–8.0 (m, 34H, Ph and Py). $^{31}P\{^1H\}$ NMR (CD_2Cl_2): δ −0.9 (d, $^2J_{pp} = 18.4$ Hz, PPh_3), 5.7 (d, $^2J_{pp} = 18.4$ Hz, PPh_3). Anal. Calc. for $C_{43}H_{38}IrNO_2P_2S$: C, 58.23; H, 4.32; N, 1.58. Found: C, 58.08; H, 4.46; N, 1.50%.

2.3.4. Preparation of $[IrH(C{\equiv}CC_6H_4CH_3)(\eta^2\text{-}SNC_5H_4)(PPh_3)_2]$ (6)

To solution of complex **2** (46 mg, 0.056 mmol) in toluene (2 mL), *p*-tolylacetylene (10 μl, 0.079 mmol) was added at room temperature. After 5 min, the solvent was removed under high vacuum and the residue was washed with hexane (3 × 5 mL) and then dried in vacuo, giving yellow powder of **6** (42 mg, 0.045 mmol, 80%). FAB mass (*m*/*z*): 942 ($[M–H]^+$). IR (KBr): 2300 (Ir–H), 2106 cm^{-1}(C≡C). ^1H NMR (C_6D_6): δ −9.56 (dd, $J_{P(trans)H} = 171$ Hz, $J_{P(cis)H} = 16.5$ Hz, 1H, Ir–H), 1.92(s, 3H, CH_3), 6.8–8.5 (m, 38H, Ph, Py). $^{31}P\{^1H\}$ NMR (C_6D_6): δ −3.9 (d, $J_{pp} = 6.9$ Hz, PPh_3), 12.2 (d, $J_{pp} = 6.9$ Hz, PPh_3).

2.4. General procedure for catalytic alkyne dimerization

The mixture of iridium complex **2** (0.030 mmol), toluene (3 mL) and terminal alkyne (1.0 mmol) charged in a sealed tube under argon. After stirring for 6 h at 80 °C, the solvent was removed and the residue was chromatographed on silica gel, using ether/hexane (1:3) as eluent. The solvent was removed to give dimeric product **7**. All products were

Table 1
Crystal data for $[Ir(\eta^2\text{-}SC_5H_4N)(PPh_3)_2]\cdot 0.5CH_2Cl_2$ (**2** · $0.5CH_2Cl_2$), $[IrCl_2(\eta^2\text{-}SC_5H_4N)(PPh_3)_2]$ (**3**) and $[IrH(SiMePh_2)(\eta^2\text{-}SC_5H_4N)(PPh_3)_2]$ (**4**)

Compound	**2** · $0.5CH_2Cl_2$	**3**	**4**
Formula	$C_{41.5}H_{35}ClIrNP_2S$	$C_{41}H_{34}NCl_2IrSP_2$	$C_{54}H_{48}NSSiP_2Ir$
Molecular weight	869.42	897.86	1025.29
Crystal color, habit	Red, prismatic	Yellow, prismatic	Yellow, block
Crystal size (mm)	0.23 × 0.05 × 0.02	0.24 × 0.14 × 0.11	0.08 × 0.08 × 0.03
Crystal system	Monoclinic	Monoclinic	Monoclinic
Space group	$P2_1/n$ (No. 14)	$P2_1/m$ (No. 11)	$C2/c$ (No. 15)
a (Å)	10.471(2)	9.4642(10)	35.4026(6)
b (Å)	29.975(5)	24.510(3)	12.1561(2)
c (Å)	11.596(3)	15.4529(17)	25.0020(5)
α (°)	90.0	90.0	90.0
β (°)	103.009(5)	90.0917(16)	123.9410(7)
γ (°)	90.00	90.0	90.0
V (Å)	3546.2(12)	3584.5(7)	8926.4(3)
Z	4	4	8
D_{calc} (g cm^{-3})	1.628	1.664	1.526
μ (Mo Kα) (cm^{-1})	40.314	40.631	–
μ (Cu Kα) (cm^{-1})	–	–	73.243
Reflections measured	22339	72781	45941
2θ (°)	55.0	60.1	136.5
Independent reflections (R_{int})	7988 (0.040)	10703 (0.091)	8172 (0.066)
Number of variables	434	464	546
Reflection/parameter ratio	18.41	23.07	14.97
Residuals: R; R_w	0.0589; 0.0811	0.0613; 0.1398	0.0357; 0.0850
Residuals: R_1	0.0421	0.0551	0.0322
Number of reflections to calculated R_1	6259 ($I > 2.0\sigma(I)$)	9163 ($I > 2.0\sigma(I)$)	7463 ($I > 2.0\sigma(I)$)
Goodness-of-fit indicator	1.197	1.162	1.066

identified by comparison of the observed chemical shifts with literature data [11].

2.5. Experimental procedure for X-ray crystallography

Suitable single crystals were obtained by recrystallization from CH_2Cl_2/diethyl ether for **2** · $0.5CH_2Cl_2$ and **4**, and toluene/hexane for **3**. Crystal of **2** · $0.5CH_2Cl_2$ and **3** were mounted at the top of nylon loop using liquid paraffin, which was set on a Rigaku Saturn CCD/Rigaku AFC 8 diffractometer. The measurement was made by using Mo Kα radiation ($\lambda = 0.7107$ Å) at −183 °C under a cold nitrogen stream. Indexing of crystals of **2** · $0.5CH_2Cl_2$ and **3** were performed from six images that were exposed for 5 s. The crystal-to-detector distances were 40.06 mm for **2** · $0.5CH_2Cl_2$ and 40.05 mm for **3**. A total of 556 oscillation for **2** · $0.5CH_2Cl_2$ and 1440 oscillation for **3** images were collected. Readout was performed in the 0.137 mm pixel mode for **2** · $0.5CH_2Cl_2$ and **3**.

Crystal of **4** was mounted at the top of nylon loop using liquid paraffin, which was set on a Rigaku RAXIS RAPID imaging plate/ultra X18 diffractometer. The data were corrected for Lorentz and polarization effects. The measurement was made by using Cu Kα radiation ($\lambda = 1.54187$ Å) at −175 °C under a cold nitrogen stream. Indexing was performed from three oscillations that were exposed for 150 s. The crystal-to-detector distance was 127.40 mm. A total of 160 oscillation images were collected. Readout was performed in the 0.100 mm pixel mode.

2.6. Determination of structure

The crystal parameters along with data collections are summarized in Table 1. These structures were solved by direct methods (SIR92) [12] for **2** · $0.5CH_2Cl_2$, (SIR2004) [13] for **3** and (SHELX97) [14] for **4** and expanded using Fourier techniques [15]. All of non-hydrogen atoms were refined anisotropically. In complex **2** · $0.5CH_2Cl_2$ and **3**, all hydrogen atoms were refined using riding model. In complex **4**, some hydrogen atoms were refined isotropically and others were refined using the riding model. All calculations were performed using the CrystalStructure [16] crystallographic software package except for refinement, which was performed using SHELXL-97 [14].

3. Results and discussion

3.1. Synthesis of iridium(I)pyridine-2-thiolate complex $[Ir(SNC_5H_4)(PPh_3)_2]$(**2**)

Iridium(I) complex **2** bearing pyridine-2-tholate was prepared by the reaction of ethylene complex $[IrCl(C_2H_4)(PPh_3)_2]$ (**1**) with lithium salt of pyridine-2-thiolate $Li[SNC_5H_4]$ in THF at −78 °C (Scheme 1).

Molecular peak of $m/z = 827$ in the FAB mass spectrometry and elementary analysis corresponded to the formula of $[Ir(SNC_5H_4)(PPh_3)_2]$. The $^{31}P\{^1H\}$ NMR spectra of **2** showed two doublets at 20.9 and 22.8 ppm ($J_{pp} = 20.4$ Hz) assigned to two PPh_3 ligands.

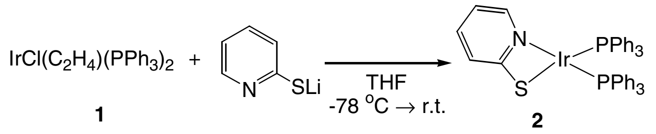

Scheme 1. Synthesis of Ir(I)pyridine-2-thiolate complex.

The structure of complex **2** was also confirmed by X-ray analysis. The ORTEP drawing of complex **2** is shown in Fig. 1. Selected bond distances and angles are listed in Table 2. The crystal contained CH_2Cl_2 in the lattice. The complex have square planar geometry around iridium metal. The sum of angles around iridium atom is 359.9°. The Ir–N and Ir–S bond distances were 2.117(4) and 2.3910(12) Å, respectively. The N–Ir–S bond angle was 68.28(12)°. The Ir–S bond distance was shorter than that for previously reported iridium(III)pyridine-2-thiolate complexes [6].

An attempted substitution of the coordinated pyridine unit of pyridine-2-thiolate ligand by the reaction of complex **2** with triphenylphosphine in refluxing toluene resulted in no reaction (recovering yield: 90%). This result showed high stability of the chelating pyridine-2-thiolate ligand in complex **2**. On the other hand, complex **2** was unstable toward air in solution and color changed from red to yellow for a few seconds.

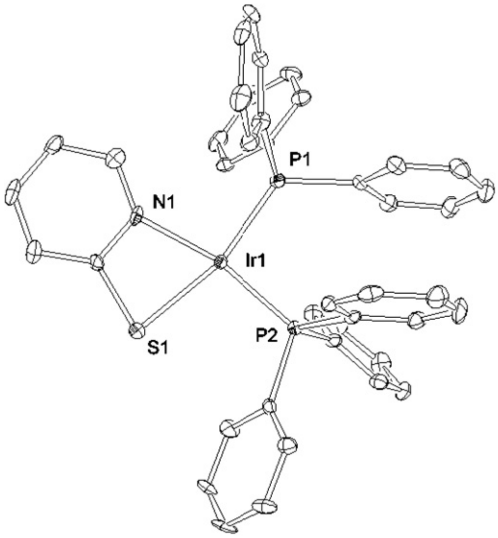

Fig. 1. ORTEP drawing of complex **2** with thermal ellipsoids drawn at the 50% probability level. Hydrogen atoms and CH_2Cl_2 molecule are omitted for clarity.

Table 2
Selected bond distances (Å) and angles (°) for $[Ir(\eta^2\text{-}C_5H_3NS)(PPh_3)_2] \cdot 0.5CH_2Cl_2$ ($\mathbf{2} \cdot 0.5CH_2Cl_2$)

Ir(1)–N(1)	2.117(4)	Ir(1)–S(1)	2.3910(12)
Ir(1)–P(1)	2.2266(12)	Ir(1)–P(2)	2.2119(14)
N(1)–Ir(1)–S(1)	68.28(12)	N(1)–Ir(1)–P(1)	96.86(12)
P(2)–Ir(1)–S(1)	98.50(4)	P(1)–Ir(1)–P(2)	96.26(5)

3.2. Reactions of iridium(I)pyridine-2-thiolate complex 2

3.2.1. Reaction of complex 2 with chloroform

The complex **2** reacted readily with chloroform at room temperature to afford the dichloro complex **3** in 47% yield (Scheme 2). The structure of complex **3** was confirmed by X-ray analysis. The ORTEP drawing of complex **3** is displayed in Fig. 2. Selected bond distances and angles are listed in Table 3. The crystal contained two independent iridium complex having Ir(1) and Ir(2). The complex has

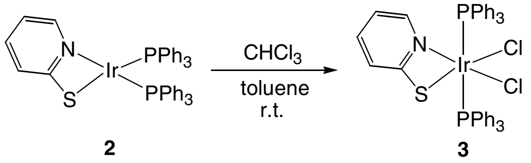

Scheme 2. Reaction of Ir(I)pyridine-2-thiolate complex with chloroform.

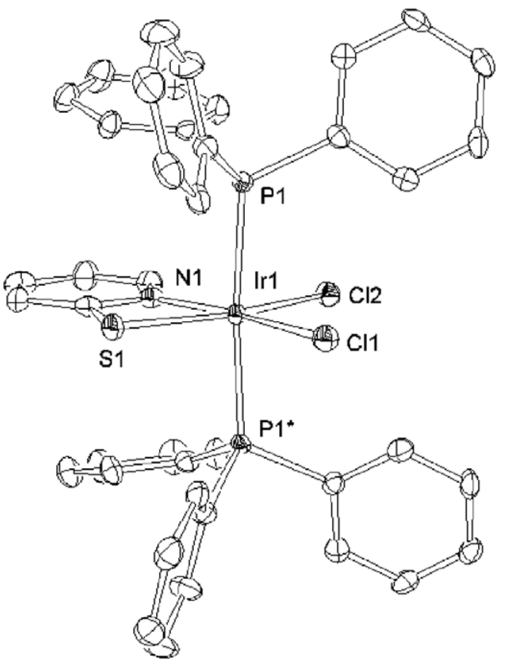

Fig. 2. ORTEP drawing of complex **3** with thermal ellipsoids drawn at the 50% probability level. All hydrogen atoms are omitted for clarity.

Table 3
Selected bond distances (Å) and angles (°) for $[IrCl_2(\eta^2\text{-}C_5H_3NS)(PPh_3)_2]$ (**3**)

Ir(1)–Cl(1)	2.405(2)	Ir(1)–Cl(2)	2.400(2)
Ir(1)–N(1)	2.051(8)	Ir(1)–S(1)	2.3988(19)
Ir(1)–P(1)	2.3452(14)	Ir(2)–Cl(3)	2.403(2)
Ir(2)–Cl(4)	2.405(2)	Ir(2)–N(2)	2.037(8)
Ir(2)–S(2)	2.391(2)	Ir(2)–P(2)	2.3447(16)
Cl(1)–Ir(1)–Cl(2)	97.64(6)	N(1)–Ir(1)–S(1)	68.0(2)
Cl(1)–Ir(1)–S(1)	101.51(7)	Cl(2)–Ir(1)–N(1)	92.8(2)
P(1)–Ir(1)–P(1*)	175.17(5)	Cl(3)–Ir(1)–Cl(4)	96.51(8)
N(2)–Ir(2)–S(2)	68.4(2)	Cl(3)–Ir(2)–S(2)	102.86(8)
Cl(4)–Ir(2)–N(2)	92.3(2)	P(2)–Ir(2)–P(2*)	176.05(8)

octahedral geometry around a iridium metal, and the pyrdine-2-thiolate ligand was located on a coplanar with two chloride ligands. Two phosphine ligands of complex **3** are located in mutually *trans* position. Ir(1)–N(1) bond distance (2.051(8) Å) of complex **3** is shorter than that for complex **2** (2.117(4) Å). These observation reflect the difference of electron density on iridium metals between iridium(III) and iridium(I). The axial P(1)–Ir(1) bond distance was longer than that for complex **2**. Other bond distances and angles of pyridine-2-thiolate ligand of complex **3** are similar to those of complex **2**.

The $^{31}P\{^1H\}$ NMR spectrum showed one singlet signal at −12.7 ppm. This result indicate the symmetrical structure of complex **3** in solution as well as structure in the solid state. The formation of dichloro complex **3** suggested the strong oxidative tendency of complex **2**.

3.2.2. Reaction of complex **2** *with methyldiphenylsilane*

On the treatment of complex **2** with methyldiphenylsilane at room temperature, oxidative addition of Si–H to iridium(I) metal was occurred and hydride-silyl complex **4** was isolated in 63% yield (Scheme 3).

The ^1H NMR spectrum of **4** showed hydride signal at −19.60 ppm as triplet with a P–H coupling constant of 16.5 Hz. The $^{31}P\{^1H\}$ NMR spectrum shows a singlet at 5.8 ppm assignable for PPh_3 ligands. The $^{31}P\{^1H\}$ NMR spectrum of complex **4** suggested that the complex **4** has a symmetrical structure with mutually *trans* phosphine ligands.

The structure of complex **4** was also confirmed by X-ray analysis. The ORTEP drawing of complex **4** is displayed in Fig. 3. Selected bond distances and angles are listed in Table 4. Two phosphine ligands of complex **4** are located in mutually *trans* position as well as complex **3**. Silyl ligand is *trans* to sulfur atom, and the hydride ligand is *trans* to nitrogen atom. Similar cationic iridium(III) hydride complex bearing pyridine-2-thiolate ligand $[IrH(\eta^2\text{-}SN\text{-}C_5H_4)(CO)(PPh_3)_2][BF_4]$ had been reported by Dahlenburg [6b]. The hydride ligand of the reported cationic complex is *trans* to sulfur atom. The crystal structure of complex **4** coincide with solution-state geometry which observed by ^1H and $^{31}P\{^1H\}$ NMR spectra.

The Ir–Si bond distance of complex **4** is 2.3810(9) Å. The bond distance is in good agreement with reported value for the normal iridium(III)–Si bond distances [17]. The Ir–N (2.172(3) Å) and Ir–S (2.5114(8) Å) bond distances of complex **4** were slightly longer than those for dichloro-iridium complex **3**.

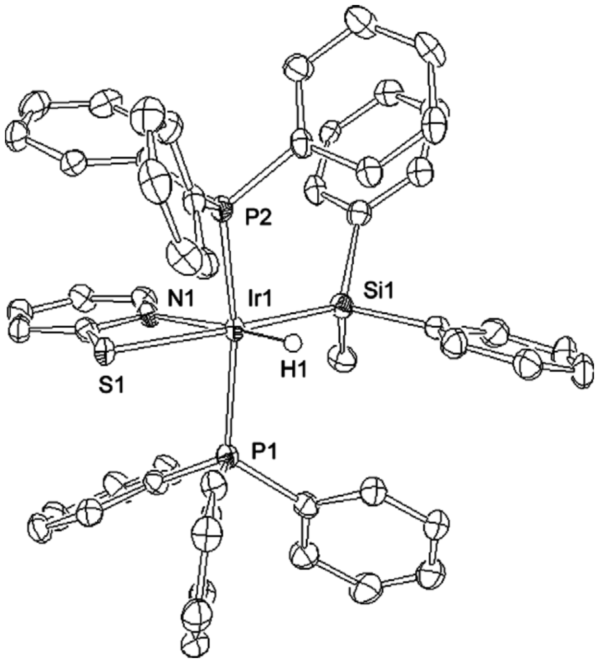

Fig. 3. ORTEP drawing of complex **4** with thermal ellipsoids drawn at the 50% probability level. Hydrogen atoms are omitted for clarity.

Table 4
Selected bond distances (Å) and angles (°) for $[IrH(SiMePh_2)(\eta^2\text{-}C_5H_3NS)(PPh_3)_2]$ (**4**)

Ir(1)–H(1)	1.50(4)	Ir(1)–N(1)	2.172(3)
Ir(1)–S(1)	2.5114(8)	Ir(1)–Si(1)	2.3810(9)
Ir(1)–P(1)	2.3501(9)	Ir(1)–P(2)	2.3059(9)
H(1)–Ir(1)–Si(1)	79.4(16)	H(1)–Ir(1)–S(1)	110.6(16)
N(1)–Ir(1)–S(1)	65.61(7)	N(1)–Ir(1)–Si(1)	104.31(8)
P(1)–Ir(1)–P(2)	163.83(3)		

3.2.3. Reaction of complex **2** *with acetic acid*

When complex **2** was treated with acetic acid at room temperature, hydride-acetate complex **5** was formed (Scheme 4). The result of elementary analysis corresponded to formula of $[Ir(CH_3COOH)(NSC_5H_4)(PPh_3)_2]$. The ^1H NMR spectrum of **5** showed hydride signal at −17.53 ppm as double doublet with a P–H coupling constant of 16.5 and 20.2 Hz. In $^{31}P\{^1H\}$ NMR spectrum of **5**, two doublets at −0.9 and 5.7 ppm with P–H coupling constants of 18.4 Hz were observed. These ^1H and $^{31}P\{^1H\}$ NMR spectra show that two phosphine ligands of complex **5** are located in mutually *cis* position and by the P–H(hydride) coupling constants ($^2J_{P1H} = 16.8$ Hz, $^2J_{P2H} =$

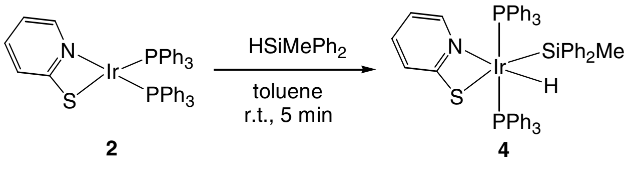

Scheme 3. Reaction of Ir(I)pyridine-2-thiolate complex with methyldiphenylsilane.

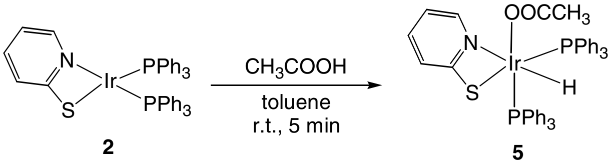

Scheme 4. Reaction of Ir(I)pyridine-2-thiolate complex with acetic acid.

20.2 Hz) of ^{1}H NMR measurement, hydride and two phosphine ligands are located in mutually *cis* position [18].

3.2.4. Reaction of complex 2with *p*-tolylacetylene

When complex **2** was treated with *p*-tolylacetylene at room temperature, hydride-acetylide complex **6** was formed (Scheme 5). Molecular peak of $m/z = 942$ in the FAB mass spectrometry corresponded to the formula of $[Ir(HC{\equiv}C(p\text{-tolyl}))(NSC_5H_4)(PPh_3)_2]–H]$. In the IR spectra, the most noticeable absorption were observed at 2300 and 2106 cm^{-1}, which were assigned to Ir–H and the C≡C vibration of acetylide ligand, respectively. The ^{1}H NMR spectrum showed hydride signal as a double doublet at −9.56 ppm with a P–P coupling constant of 16.5 and 171 Hz was observed. The coupling constant of 171 Hz indicate that hydride locate in the *trans* to PPh$_3$ ligand [6a]. In $^{31}P\{^1H\}$ NMR spectrum of **6**, two doublets assignable to mutually *cis* phosphine ligands at −3.9 and 12.2 ppm with P–H coupling constants of 6.9 Hz were observed. These spectroscopic results indicate that structure of **6** is **6A** or **6B** as shown in Scheme 5. The similar hydride-acetylide complex of iridium(III) bearing acetylacetonato complex $[IrH(C{\equiv}CR)(\eta^2\text{-acac})(PPh_3)_2]$ (R = Ph, Cy, SiMe$_3$) has been reported [17]. In case of the acetylacetonato complex, two phosphine ligands located in mutually *trans* position.

3.3. Alkyne dimerization reaction catalyzed by iridium(I) complex 2

The transition-metal-catalyzed dimerization of alkynes has received much attention as a useful method for the synthesis of substituted enynes [19]. Many late transition metal complexes such as ruthenium [20], rhodium [21], iridium [22], nickel [23], and palladium [24] have been used in the dimerization of alkynes. Miyaura et al. reported that $[IrCl(COD)]_2/PR_3$ system catalyzed head-to-head dimerization of terminal alkynes leading to enynes with high stereoselectivity [11b]. However, iridium-catalyzed dimerization has not been well examined other than $[IrCl(COD)]_2$/phosphine system. Accordingly, we investigated alkyne dimerization by using iridium(I) complex **2** (Scheme 6).

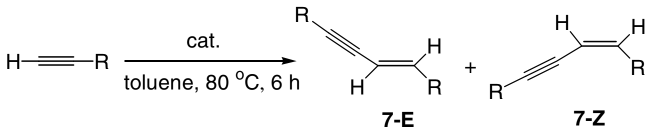

Scheme 6. Catalytic dimerization of terminal alkyne.

Table 5
Results of catalytic dimerization reaction catalyzed by complex **2**[a]

Entry	R	Yield (%)[b]	Ratio (**7-E**/**7-Z**)[c]
1	*p*-toly	72	92:8
2	Ph	65	91:9
3	^{n}Bu	42	91:9
4	^{t}Bu	54	95:5
5	TMS	55	100:0

[a] Reaction conditions; alkyne (1.0 mmol), complex **2** (0.03 mmol), toluene (3 mL), temperature (80 °C), reaction time (6 h).

[b] Isolated yields.

[c] Determined by ^{1}H NMR measurement.

The results and reaction conditions are listed in Table 5. In the presence of complex **2**, head-to-head dimerization of *p*-tolylacetylene or phenylacetylene proceeded with high *E*-selectivity (entries 1 and 2). In this reaction, coupling by-products such as head-to-tail dimerization products and trimerization products were not generated. In case of bimetallic pyridine-2-thiolate catalytic system ($[Ir(\mu\text{-}SNC_5H_4)(COD)]_2/2PPh_3$), dimerization of *p*-tolylacetylene proceeded in low yield (36%) with low stereoselectivity ($E/Z = 65{:}35$). These results clearly demonstrated that the use of bidentate pyridine-2-thiolate complexes enables high *E*-selectivity. The complex **2** also showed moderate activity and high *E*-selectivity for dimerization of alkylacetylene (entries 3 and 4) and trimethylsilylacetylene (entry 5).

The possible pathway for the formation of dimerization product **7** is shown in Scheme 7. An oxidative addition of the alkyne C–H bond to iridium(I) affords hydride-acetylide complex **6**. Addition of the iridium hydride to the another alkyne then provides intermediate **A**. It is probably prefer to form E-type intermediate **A** due to the fact that **A** has a stable structure to avoid steric repulsion between alkene unit and other ligands around iridium metal. Reductive elimination furnishes enyne **7-E**, and regenerates the hydride-acetylide complex **6**. Recently, mechanistic study for dimerization of terminal alkynes in iridium complex bearing PCP pincer ligand had been reported by Goldman et al. [25], which showed that alkyne insertion into Ir–H bond followed by reductive elimination affords an enyne.

4. Summary

A novel iridium(I) complex bearing chelating pyridine-2-thiolate ligand was prepared. The complex was readily

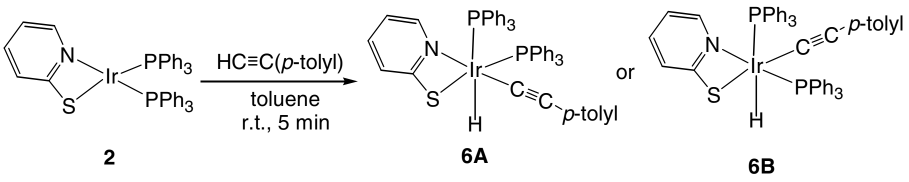

Scheme 5. Reaction of Ir(I) pyridine-2-thiolate complex with *p*-tolylacetylene.

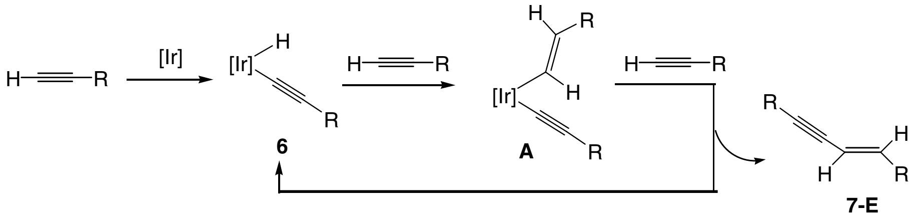

Scheme 7. Possible pathway for catalytic dimerization of alkyne catalyzed by complex **2**.

reacted with chloroform, methyldiphenylsilane, acetic acid and alkyne to give iridium(III) complexes. Two phosphine ligands of hydride-acetate and hydride-acetylide complex were mutually *cis* position whereas for dichloro-complex and hydride-silyl complex, phosphine ligands were positioned mutually *trans*. The iridium(I) complex was active for catalytic dimerization of terminal alkynes, which proceeded with high *E*-selectivity. Further investigation of reactivity of these complexes is underway in our laboratory.

Acknowledgements

The authors are grateful to Dr. Noriyuki Suzuki and Daisuke Hashizume (RIKEN) for their kind help in X-ray measurement.

Appendix A. Supplementary material

CCDC 646693, 646694 and 646695 contain the supplementary crystallographic data for **2**, **3** and **4**. These data can be obtained free of charge via http://www.ccdc.cam.ac.uk/conts/retrieving.html, or from the Cambridge Crystallographic Data Centre, 12 Union Road, Cambridge CB2 1EZ, UK; fax: (+44) 1223-336-033; or e-mail: deposit@ccdc.cam.ac.uk. Supplementary data associated with this article can be found, in the online version, at doi:10.1016/j.jorganchem.2007.06.030.

References

[1] (a) E.R. Raper, Coord. Chem. Rev. 153 (1996) 199;
(b) E.R. Raper, Coord. Chem. Rev. 165 (1997) 475.
[2] (a) K. Umakoshi, A. Ichimura, I. Kinoshita, S. Ooi, Inorg. Chem. 29 (1990) 4005;
(b) E.C. Constable, A.C. King, C.A. Palmer, P.R. Raithby, Inorg. Chem. Acta 184 (1991) 43.
[3] (a) P.D. Cookson, E.R.T. Tiekink, J. Chem. Soc., Dalton Trans. (1993) 259;
(b) P. Aslanidis, S.K. Hadgikakou, P. Karagiannidis, B. Kojicprodic, M. Luic, Polyhedron 13 (1994) 3119;
(c) C. Vetter, C. Wagner, J. Schmidt, D. Steinborn, Inorg. Chim. Acta 359 (2006) 4326.
[4] (a) Y. Nakatsu, Y. Nakamura, K. Matsumoto, S. Ooi, Inorg. Chim. Acta 196 (1992) 81;
(b) M. Gupta, R.E. Cramer, K. Ho, C. Pettersen, S. Mishina, J. Belli, C.M. Jensen, Inorg. Chem. 34 (1995) 60;
(c) A.S. Pedrares, M.L. Durán, J. Romero, J.A.G. Vázquez, J.C. Monteagudo, A. Sousa, J.R. Dilworth, Inorg. Chim. Acta 359 (2006) 863.
[5] (a) M.A. Ciriano, J.J.P. Torrente, F. Viguri, F.J. Lahoz, L.A. Oro, A. Tiripicchio, M.T. Camellini, J. Chem. Soc. Dalton Trans. (1990) 1493;
(b) J.G. Reynolds, S.C. Sendlinger, A.M. Murray, J.C. Huffman, G. Christou, Angew. Chem. Int. Ed. Engl. 31 (1992) 1253;
(c) R.M. Tylicki, W. Wu, P.E. Fanwick, R.A. Walton, Inorg. Chem. 34 (1995) 988;
(d) E.W. Ainscough, A.M. Brodie, R.K. Coll, T.G. Kotch, A.J. Lees, A.J.A. Mair, J.M. Waters, J. Organomet. Chem. 517 (1996) 173.
[6] (a) S. Park, A.J. Lough, R.H. Morris, Inorg. Chem. 35 (1996) 3001;
(b) L. Dahlenburg, M. Kühnlein, Eur. J. Inorg. Chem. (2000) 2117.
[7] Y. Sekioka, S. Kaizaki, J.M. Mayer, T. Suzuki, Inorg. Chem. 44 (2005) 8173.
[8] M.A. Ciriano, F. Viguri, L.A. Oro, A. Tiripicchio, M.T. Camellini, Angew. Chem. Int. Ed. Engl. 26 (1987) 444.
[9] V.M. Soto, J.J.P. Torrente, L.A. Oro, F.J. Lahoz, M.L. Martín, M.P. Hake, D.B. Grotjahn, Organometallics 25 (2006) 4374.
[10] A. van der Ent, A.L. Onderdelinden, Inorg. Chim. Acta 7 (1973) 203.
[11] (a) C.S. Yi, N. Lin, Organometallics 15 (1996) 3968;
(b) T. Ohmura, S. Yorozuya, Y. Yamamoto, N. Miyaura, Organometallics 19 (2000).
[12] SIR92: A. Altomare, G. Cascarano, C. Giacovazzo, A. Guagliardi, M. Burla, G. Polidori, M. Camalli, J. Appl. Crystallogr. 27 (1994) 435.
[13] SIR2004: M.C. Burla, R. Caliandro, M. Camalli, B. Carrozzini, G.L. Cascarano, L. De Caro, C. Giacovazzo, G. Polidori, R. Spagna (2005).
[14] SHELX97: G.M. Sheldrick, 1997.
[15] DIRDIF99: P.T. Beurskens, G. Admiraal, G. Beurskens, W.P. Bosman, R. de Gelder, R. Israel, J.M.M. Smits, The DIRDIF-99 program system, Technical Report of the Crystallography Laboratory, University of Nijmegen, The Netherlands, 1999.
[16] Crystal Structure 3.8.0: Crystal Structure Analysis Package, Rigaku and Rigaku/MSC (2000–2006). 9009 New Trails Dr. The Woodlands, TX 77381, USA.
[17] M.A. Esteruelas, F.J. Lahoz, E. Oñate, L.A. Oro, L. Rodríguez, Organometallics 15 (1996) 823.
[18] J.A. van Doorn, C. Masters, C. van der Woude, J. Chem. Soc., Dalton 1213 (1978).
[19] B.M. Trost, Science 254 (1991) 1471.
[20] (a) For ruthenium-catalyzed dimerization of alkynes, see: Y. Sasaki, P.H. Dixneuf, J. Chem. Soc., Chem. Commun. (1986) 790;
(b) C. Bianchini, M. Peruzzini, F. Zanobini, P. Frediani, A. Albinati, J. Am. Chem. Soc. 113 (1991) 5453;
(c) L. Dahlenburg, K.-M. Frosin, S. Kerstan, D. Werner, J. Organomet. Chem. 407 (1991) 115;
(d) A.M. Echavarren, J. Lopez, A. Santos, J. Montoya, J. Organomet. Chem. 414 (1991) 393;
(e) C. Bianchini, M. Peruzzini, F. Zanobini, P. Frediani, A. Albinati, J. Am. Chem. Soc. 113 (1991) 5453;
(f) C. Bianchini, P. Frediani, D. Masi, M. Peruzzini, F. Zanobini, Organometallics 13 (1994) 4616;
(g) C.S. Yi, N. Liu, A.L. Rheingold, L.M.L. Sands, Organometallics 15 (1996) 5275;
(h) J.-P. Gü, D. Masui, Y. Ishii, M. Hidai, Chem. Lett. (1998) 1003;

(i) K. Melis, D.D. Vos, P. Jacobs, F. Verpoort, J. Organomet. Chem. 659 (2002) 159;

(j) Y. Gao, R.J. Puddephatt, Inorg. Chim. Acta 350 (2003) 101;

(k) H. Katayama, H. Yari, M. Tanaka, F. Ozawa, Chem. Commun. (2005) 4336, and [11a].

[21] (a) For recent example of rhodium-catalyzed dimerization of alkynes, see: J. Ohshita, K. Furumori, A. Matsuguchi, M. Ishikawa, J. Org. Chem. 55 (1990) 3277;

(b) I.P. Kovalev, K.V. Yevakov, Y.A. Strelenko, M.G. Vinogradov, G.I. Nikishin, J. Organomet. Chem. 386 (1990) 139;

(c) W.T. Boese, A.S. Goldman, Organometallics 10 (1991) 782;

(d) M. Schäfer, N. Mohr, J. Wolf, H. Werner, Angew. Chem., Int. Ed. Engl. 32 (1993) 1315;

(e) C.-C. Lee, Y.-C. Lin, Y.-H. Liu, Y. Wang, Organometallics 24 (2005) 136;

(f) W. Weng, C. Guo, R. Celenligil-Cetin, B.M. Foxman, O.V. Ozerov, Chem. Commun. (2006) 197.

[22] (a) For iridium-catalyzed dimerization of alkynes, see: C.-H. Jun, Z. Lu, R.H. Crabtree, Tetrahedron Lett. 34 (1992) 7119;

(b) T. Hirabayashi, S. Sakaguchi, Y. Ishii, Adv. Synth. Catal. 347 (2005) 872, and Ref. [11b].

[23] (a) For Nickel-catalyzed dimerization of alkynes, see: G. Giacomelli, F. Marcacci, A.M. Caporusso, L. Lardicci, Tetrahedron Lett. (1979) 3217;

(b) M. Ishikawa, J. Ohshita, Y. Ito, A. Minato, J. Chem. Soc., Chem. Commun. (1988) 804;

(c) S. Ogoshi, M. Ueta, M. Oka, H. Kurosawa, Chem. Commun. (2004) 2732.

[24] (a) For palladium-catalyzed dimerization of alkynes, see: H. Singer, G. Wilkinson, J. Chem. Soc., A (1968) 190;

(b) E.T. Sabourin, J. Mol. Catal. 26 (1984) 363;

(c) F.A. Selimov, O.G. Rutman, U.M. Dzhemilev, J. Organomet. Chem. 346 (1988) C58.

[25] R. Ghosh, X. Zhang, P. Achord, T.J. Emge, K.K. Jespersen, A.S. Goldman, J. Am. Chem. Soc. 129 (2007) 853.